Earth Reinforcement, Ochiai, Yasufuku & Omine (eds)© 1996 Balkema, Rotterdam. ISBN 90 5410 833 9

Short and long term behaviour of geogrids under static and cyclic load

Nicola Moraci
University of Reggio Calabria, Italy

Filippo Montanelli
Tenax SpA, Italy

ABSTRACT: This paper deals with the short and long term mechanical behaviour of two geogrids for soil reinforcement applications. The short term mechanical behaviour has been investigated by means of tensile tests carried out at constant rate of strain and by cyclic tests with incremental loads. The long term behaviour of these materials has been studied by means of tensile creep tests. On the base of the tests' results, the authors have proposed very simple laws to predict the behaviour of the long term deformation and tensile creep modulus. The use of the above laws has allowed the prediction of the long term deformation from the short term tests performed using cyclic loading, once the design load and the temperature are known.

1 INTRODUCTION

The principal factors affecting the mechanical behaviour of the geosynthetics for soil reinforcement applications are the following:

1. Polymer type and polymeric structure;
2. Geosynthetic structure (such as woven or nonwoven geotextile, extruded or woven geogrids);
3. Applied tensile load;
4. Service temperature;
5. Vertical confining stress and soil type;
6. Service life.

The testing program has investigated the influence on the short and long term mechanical behaviour of several parameters such as the polymer type, the geosynthetic structure, the load level and the temperature. The behaviour of two geogrids has been investigated: an HDPE extruded geogrid and a PET woven geogrid; the properties of which are reported in table 1.

Table 1: Nominal characteristics of the geogrids.

Sample	Polymer	μ g/m²	T_{max} kN/m	ε_{max} %
GE-TEN	HDPE	750	80	13.0
GT-FOR	PET	500	80	12.5

2 SHORT TERM TEST RESULTS

The tests performed have been single rib (GRI-GG1:1987) and wide width monotonic tensile tests (ISO 10319). The results are reported in table 2.

The tests have been performed in a conditioned environment at 20°C e 40° C.

Table 2: Monotonic tensile test results

Test method	GRI-GG1		ISO 10319	
Sample	GE-TEN		GE-TEN	GT-FOR
Temp, °C	20	40	20	20
T_{max}, kN/m	86.1	61.6	91.8	85.3
ε_{max}, %	13.7	17.0	14.4	12.4
$J_{sec0,2}$, kN/m	1507	928	1642	803
$J_{sec0,5}$, kN/m	1040	694	1107	465

In addition, cyclic tests with incremental loads have been performed using a hydraulic press, controlled by an Instron 8580 digital multi-axis servohydraulic controller.

In figure 1 are shown the curves related to the cyclic tests carried out on the HDPE geogrid (GE-TEN). The curves show that an unrecoverable strain appears even for low tensile levels. This viscoplastic strain increases with the testing temperature. The elastic portion (ε_{el}) of the total strain (ε_t) has been determined for the testing temperatures and the applied load, (expressed in percentage of the nominal peak value T_{max}), (table 3).

The results have shown that the ratio $\varepsilon_{el}/\varepsilon_t$ is quite constant; ranging between 64 and 72%. Both the total and elastic strain increase proportionally when increasing the temperature from 20°C to 40°C (figure 3).

In figure 2 are shown the curves related to the cyclic tests performed on the GT-FOR geogrid.

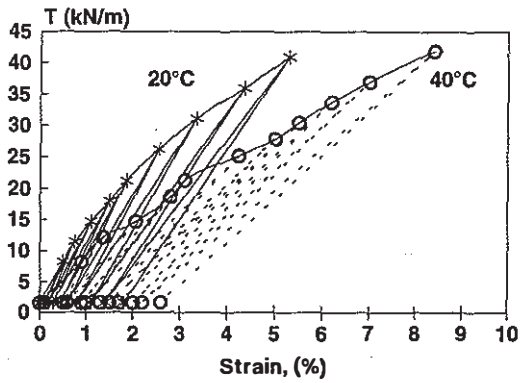

Figure 1 - Cyclic tests on the GE-TEN geogrid

Table 3: Cyclic test results on the GE-TEN geogrid.

Load,(% of T_{max})		15%	25%	35%	40%
ε_t (%)	20°C	0.81	1.71	2.86	3.58
ε_{el} (%)	20°C	0.58	1.17	1.93	2.37
ε_t (%)	40°C	1.43	2.96	5.04	5.85
ε_{el} (%)	40°C	0.91	2.00	3.54	3.98

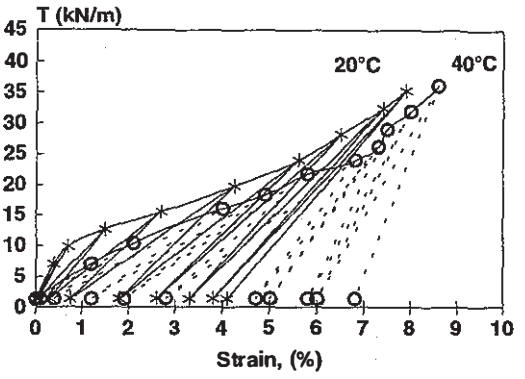

Figure 2 - Cyclic tests on the GT-FOR geogrid.

From figure 2 it is possible to observe an inflection point at a strain of about 4% at 20°C and 6% at 40°C. Before these inflection points, the tensile stiffness is relatively low. After the inflection points, the PET geogrid shows a strain hardening behaviour with a corresponding increasing tensile stiffness.

The unrecoverable strains are present even for the GT-FOR geogrids and they increase with the temperature. The elastic and the total strain are reported for the different loads and temperatures in table 4.

For the GT-FOR geogrid, the ratio $\varepsilon_{el}/\varepsilon_t$ is function of the temperature and the applied loads. In particular the elastic strain decreases as temperature increases (figure 3).

Table 4: Cyclic test results on the GT-FOR geogrid.

Load,(% of T_{max})		15%	25%	35%	40%
ε_t (%)	20°C	1.35	4.30	6.50	7.30
ε_{el} (%)	20°C	0.85	2.39	3.20	3.90
ε_t (%)	40°C	2.66	5.32	7.42	8.00
ε_{el} (%)	40°C	2.00	3.06	1.77	2.00

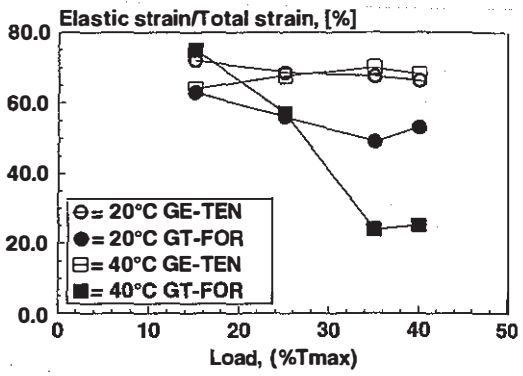

Figure 3 - Trend of the ratio $\varepsilon_{el}/\varepsilon_t$ versus load.

The secant tensile stiffnesses obtained from the standard monotonic tests are typically greater than the ones obtained from the envelope cap curves of the cyclic tests. This increase is about 20÷27% for the GE-TEN geogrid; while for the GT-FOR geogrids is about 38÷19% respectively at 20°C and at 40°C (table 5).

For the GE-TEN geogrid, the temperature plays an important role in determining the tensile stiffness.

A reduction between 12 and 34% can be calculated with increasing the temperature from 20 to 40°C. The larger changes were determined for the 2% secant tensile stiffness ($J_{sec0,2}$).

Table 5: Secant tensile stiffness for both geogrids.

	$J_{sec0,2}$, (kN/m)		$J_{sec0,5}$,(kN/m)	
GE-TEN	20°C	40°C	20°C	40°C
Monotonic test	1507	928	1040	694
Cyclic test	1100	730	790	695
GT-FOR	20°C	40°C	20°C	40°C
Monotonic test	803	-	465	-
Cyclic test	500	-	376	-

The two types of geogrid have a different behaviour in terms of tensile stiffness. The tensile stiffness of the GT-FOR geogrid is lower than the one of the GE-TEN geogrid, especially for strains lower than 4% (figure 4). At 40°C, the difference in tensile stiffness decreases.

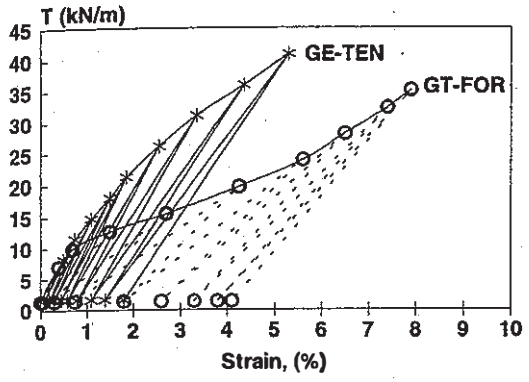

Figure 4 - Comparison between the envelope cap curves for the cyclic tests on GE-TEN and GT-FOR geogrids at 20°C.

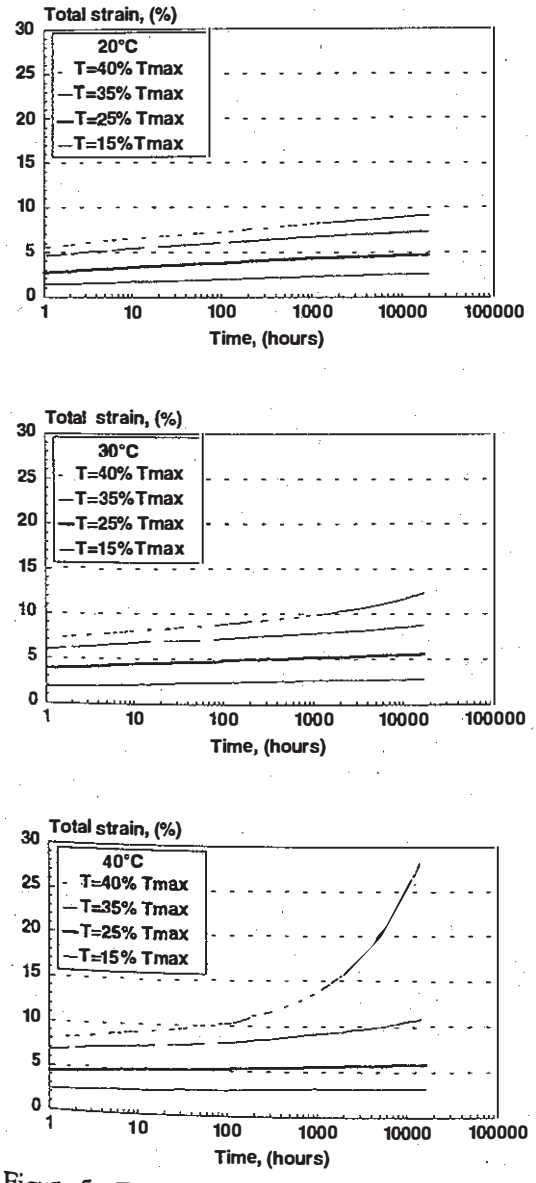

Figure 5 - Tensile creep tests on GE-TEN geogrid.

3 LONG TERM TEST RESULTS

The tensile creep tests have been carried out in agreement with the ASTM D5262 and with the existing ISO and CEN draft standards. The tests have been performed at 20°C, 30°C and 40°C using loads applied by mean of dead weights. The ratios of the applied load versus the tensile strength (T_{max}) have been 15%, 25%, 35% and 40% for the GE-TEN geogrid, and 40% and 60% for the GT-FOR geogrid. In figure 5 are reported the tensile creep test results on the extruded HDPE geogrid and in figure 6 are shown the isochronus tensile creep curves.

From the above figures, it can be noticed that at 20°C the curves show an homotetic behaviour within the testing period (2 years). At 30°C, the

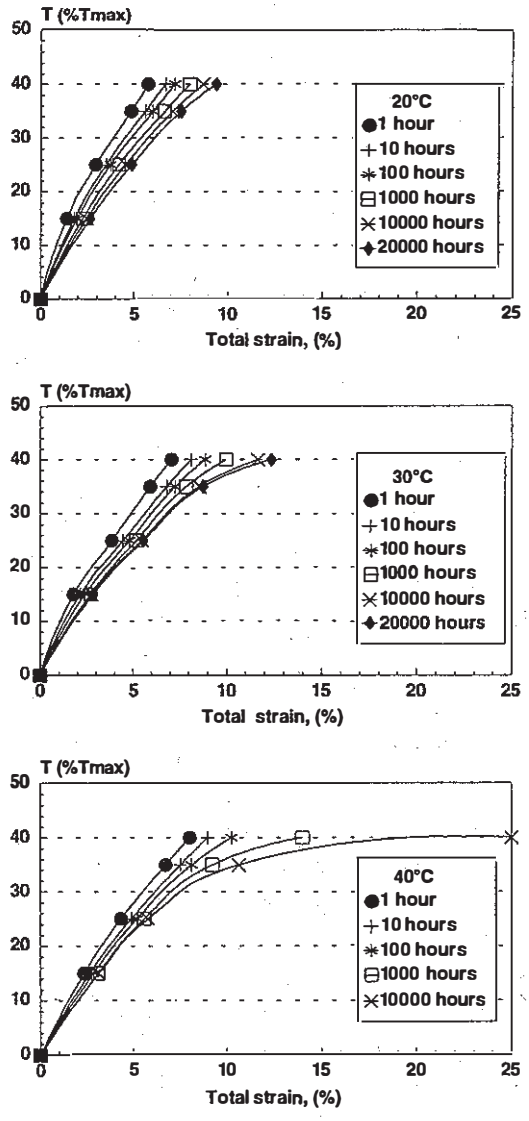

Figure 6 - Isochronus tensile creep curves at 20°C, 30°C and 40°C for geogrid GE-TEN.

curves show a linear behaviour in the log scale up to a load equal to 35% of T_{max}. This trend is shown at lower loads at 40°C. At 40°C and 40% of T_{max}, a typical tertiary creep curve is shown until specimen rupture occurs. These results show how the tertiary creep phenomena are function of the applied load and temperature.

In figure 6 are shown the isochronus tensile creep curves obtained by elaborating the tests. The steepness of these curves gives the tensile creep modulus (figure 7).

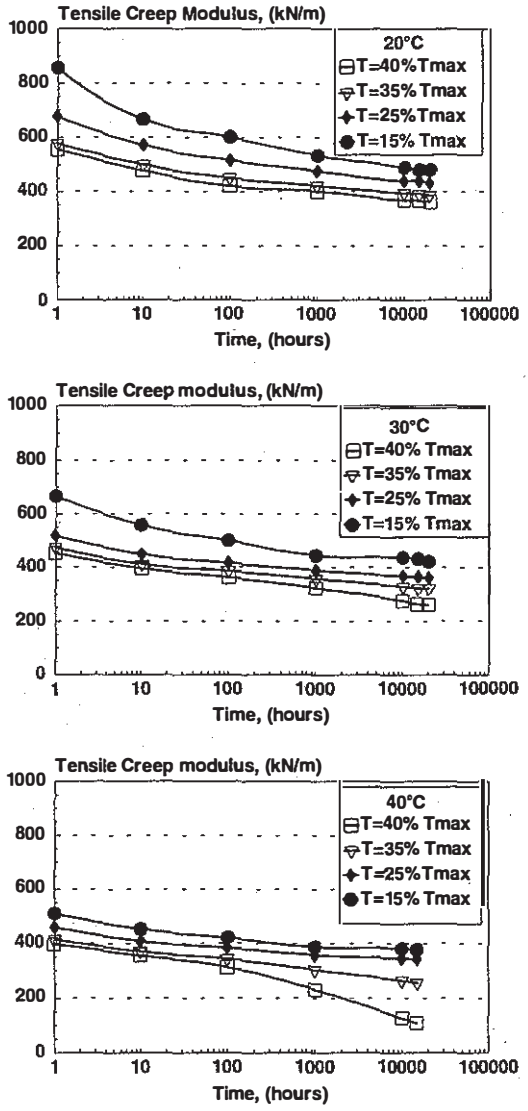

Figure 7 - Tensile creep modulus curves at 20°C, 30°C and 40°C for geogrid GE-TEN.

The curves in figure 7 show that the tensile creep modulus is decreasing with the time.

In figure 8 are reported the tensile creep tests performed on the PET woven geogrid GT-FOR.

The results show a secondary creep behaviour with a corresponding high initial strain. This behaviour yields small variations in terms of tensile creep modulus.

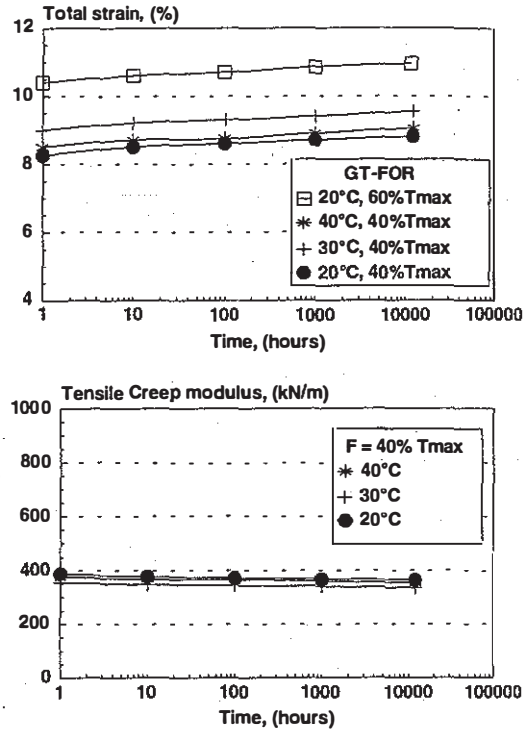

Figure 8 - Tensile creep curves at 20°C, 30°C and 40°C for GT-FOR geogrid.

The above data show that the PET geogrids have a lower viscous behaviour than the extruded HDPE geogrids. Otherwise, for the woven PET geogrid, the structural deformations are a large amount of the total strain. Thus the PET geogrids are sensible to structural deformations and the long term total strain is very similar to the HDPE geogrids.

Thus the viscous elastic behaviour of the HDPE geogrid will be analysed in the following paragraph, being the structural deformation behaviour of the PET geogrids investigated in this paragraph.

4 EXTRUDED HDPE GEOGRID LONG TERM BEHAVIOUR

The long term creep test results have been normalised in respect to the elastic deformation ε_{el} measured by means of the short term cyclic tests with incremental loads (figure 9) for the different temperatures and loads. In these diagrams the secondary creep behaviour is represented by a linear trend of the ratio $\varepsilon_{tot}/\varepsilon_{el}$ vs. long time. The regression lines can be expressed by the following relationship:

$$\varepsilon_{tot}(t) / \varepsilon_{el} = a + m \times \log(t) \quad (1)$$

where "a" and "m" are respectively the ratio of the strain ($\varepsilon_{tot}/\varepsilon_{el}$) at t=1 hour and the slope of the regression line (figure 10).

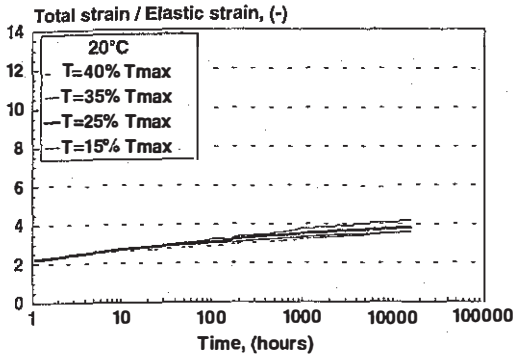

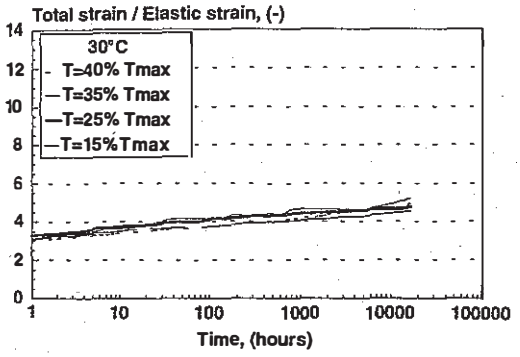

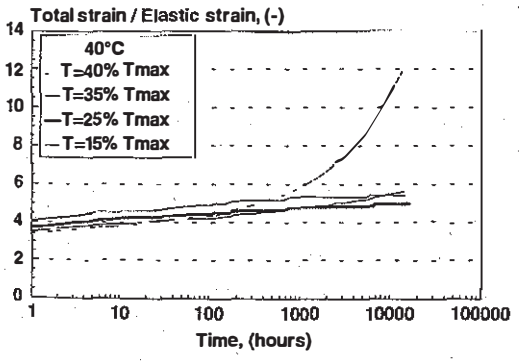

Figure 9 - Normalised tensile creep curves for the GE-TEN geogrid at 20°C, 30°C and 40°C.

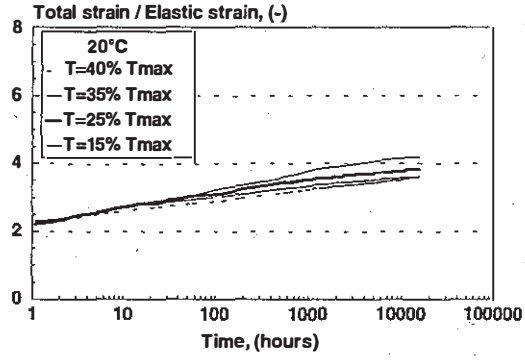

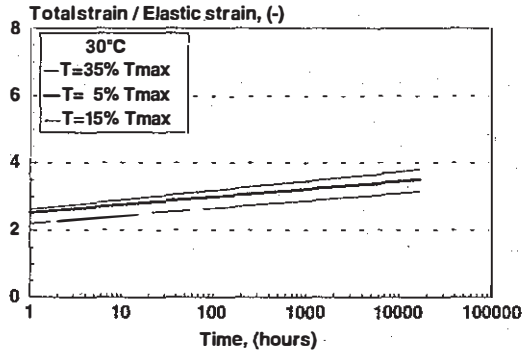

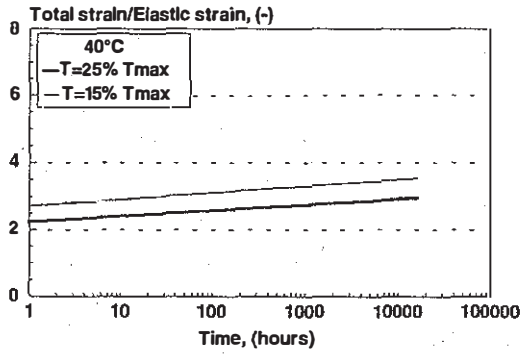

Figure 10 - Regression lines for the geogrid GE-TEN at 20°C, 30°C and 40°C.

The constants of the equation (1) are function of the applied load and temperature. Their respective values are given in table 6.

Table 6: Coefficients of the regression lines for GE-TEN geogrids.

Load, % T_{max}		15%	25%	35%	40%
m	20°C	0.471	0.369	0.306	0.323
a	20°C	2.272	2.341	2.379	2.242
m	30°C	0.282	0.233	0.226	*
a	30°C	2.618	2.528	2.199	*
m	40°C	0.183	0.153	*	*
a	40°C	2.758	2.287	*	*

* eq. (1) is not applicable.

From the above regression law, it is possible to determine, once the elastic deformations ε_{el} are known (for a given load and temperature), the total creep strain ε_{tot} at a certain time "t". Thus it is possible to determine from the short term tests the long term strain for the HDPE geogrid.

In figure 11, the trends of the tensile creep modulus ($J(t)=T/\varepsilon(t)$) are reported for several applied loads and temperatures. The following regression curve for the tensile creep modulus at t>1 hour has been obtained, within the ranges of secondary creep behaviour. (Table 7)

$$J(t) = J_1 \times t^{-n} \qquad (2)$$

where:

J_1 = tensile creep modulus at t=1 hour (kN/m);

n = exponent of the tensile creep modulus;

t = time (hour)

Table 7: Empirical values of "J_1" and "n".

Load, % T_{max}		15%	25%	35%	40%
J_1	20°C	861.1	731.2	608.1	580.6
n	20°C	0.061	0.055	0.045	0.050
J_1	30°C	633.1	505.9	458.0	*
n	30°C	0.044	0.036	0.032	*
J_1	40°C	494.6	447.9	*	*
n	40°C	0.030	0.030	*	*

* eq (2) is not applicable

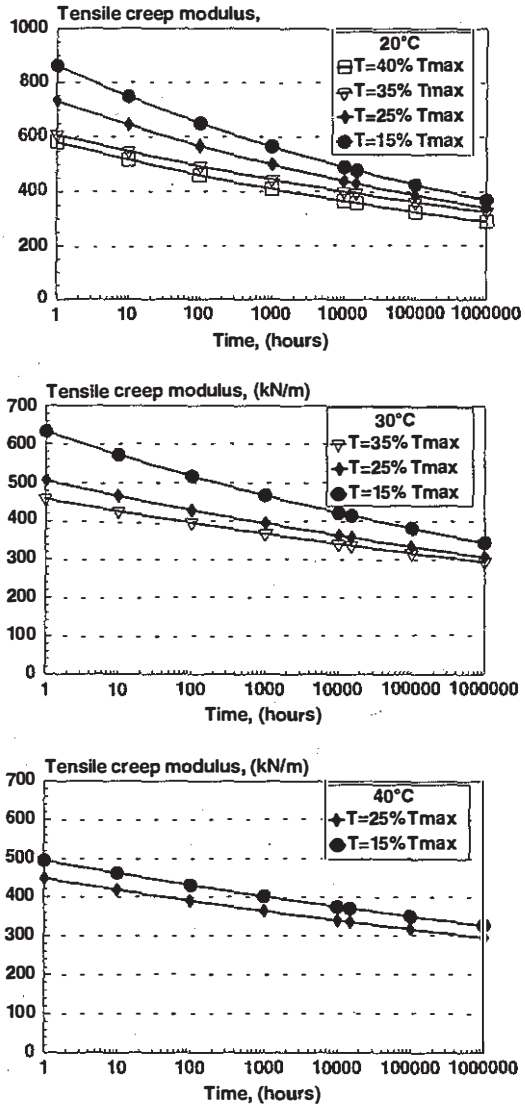

Figure 11 - Tensile creep modulus regression curves for GÉ-TEN geogrid at 20°C, 30°C and 40°C.

From equation (2) it is possible, during secondary creep conditions, to determine the tensile creep modulus J(t) once the applied load and temperatures are known. From the tensile creep modulus it is possible to determine the corresponding long term strain.

5 CONCLUSIONS

The following general conclusions can be drawn:

- the elastoviscoplastic behaviour of the woven PET geogrid is function of the geosynthetic structure and the applied load. This geosynthetic has the highest portions of total and plastic strain due to structural deformations and the lowest portion of viscous strain due to the polymer type. The testing temperature has given minor variations on the behaviour of the material. The tensile stiffness is relatively low for strain up to 4% ÷ 6% (depending on testing temperature) afterward it increases;
- particular attention shall be given to the structural deformation of the woven geogrids. The fibers' alignment and flow, the structure crimp determine up to 75% of the total deformation. The PET fibers are less sensible to creep and thus the structure deformations can be immediately measured;
- the viscoelastic behaviour of the extruded HDPE geogrids is function of the applied load and temperature. The long term strains were viscoelastic strains, since the specimens were recovering to the initial gage length once the loads were removed. This geogrid has the highest elastic strain and viscous strain. In particular can be noticed a decrease in the tensile stiffness and increase in creep strain as temperature and loads increase;
- for the extruded HDPE geogrids, the normalized creep curves ($\varepsilon_{tot}(t) / \varepsilon_{el}$) show a linear behaviour in the log time scale (table 6). This relationship is valid within the range of 40%,T_{max} at 20°C and 25%, T_{max} at 40°C;
- the tensile creep modulus curves can be represented by an exponential regression law within the ranges given here above (table 7).

The above conclusions are valid without soil confinement, being these tests performed in "isolation" conditions. It is known that lower deformations can be measured while testing the geosynthetics in interaction with soil. Thus the given strain results shall be considered as upper boundary of the ones that can be obtained in actual conditions.

REFERENCES

Montanelli F., Rimoldi P. 1993. Creep and accelerated creep testing for geogrids and geotextiles. *Proceeding Geosynthetics '93.* Vancouver, Canada.

Moraci N., Rimoldi P. 1994. Le funzioni di rinforzo e separazione. *Seminario SILP Le Applicazioni dei Geosintetici nell'Ingegneria Civile.* Padova, Italy.

Ward I.M. 1990. Mechanical properties of solid polymers. *John Wiley & Sons.* UK.